

### Realization of WDM on Chips

In optical communications, the ability to guide multiple signals within a single waveguide greatly improves the efficiency of signal transmission. This is the primary function of a wavelength division multiplexer (WDM). In the past decade, high-bandwidth wavelength division multiplexers (WDM) have shrunk a few orders of magnitude from passive fiber optic communication networks (~meters) down to photonic integrated circuits (~millimeters).

In telecommunications, there are two commonly used wavelength windows where the attenuation in fiber optic cables is lowest: 1280 - 1310 nm and 1480 - 1575 nm. These windows are shown in Figure 1 below.

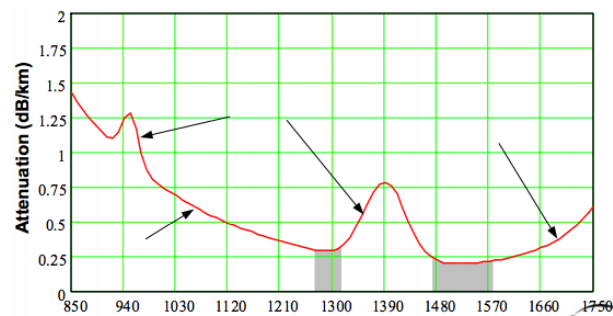


Figure 1: Attenuation of light in fused silica fiber optical cables. Even though photonic integrated circuits are not made of fused silica, they are usually connected to fiber optics and therefore responsible for transmitting at these frequencies. Figure obtained from source [1].

Using these available windows, engineers have developed the following classification for WDM, coarse WDM (CWDM) and dense WDM (DWDM), see Figure 2 below.

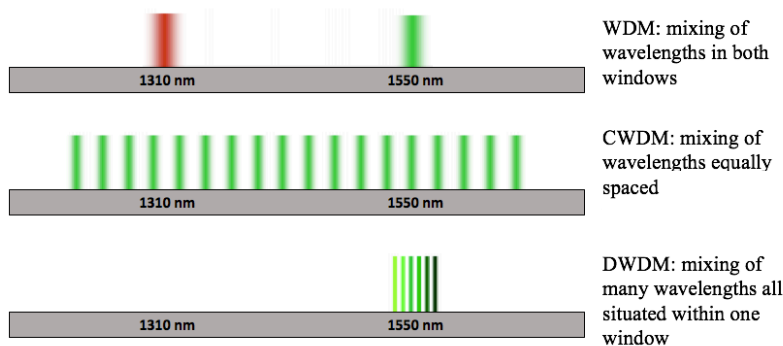
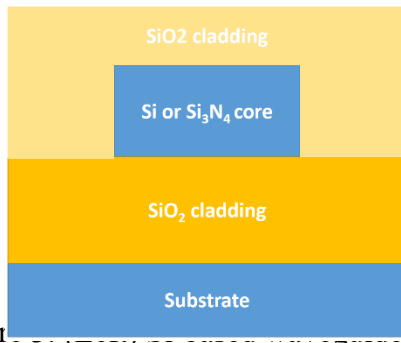


Figure 2: Optical communication classification of different types of wavelength multiplexing.

InP and Si are the two most popular materials for building photonic integrated circuits (PICs), both have been successfully implemented to make WDMs. Both indium phosphide (InP) and silicon (Si) can be used to make slab dielectric waveguides, where the core has a refractive index higher than the surrounding cladding which allows for the propagation of light via total internal

reflection. Both InP and Si PICs are promising in various applications, each with their own pros and cons. Due to silicon's indirect band-gap, laser implementation is more difficult than in its direct-gap InP counterpart. However, Si chips have the flexibility to implement polarizers and wave plates, whereas InP systems have more difficulty in this area [2]. For simplicity, we will primarily restrict this discussion to Si-based PICs, where Si ( $n \sim 3.45$ ) or  $\text{Si}_3\text{N}_4$  ( $n \sim 2$ ) is used as the propagation core and  $\text{SiO}_2$  ( $n \sim 1.5$ ) is used as the cladding. The higher-index contrast given by Si may seem beneficial as it would lead to greater optical confinement; however, it's been shown that  $\text{Si}_3\text{N}_4$  is a stronger choice for multiplexing circuit elements since the Si waveguide's refractive index is sensitive to variations in the fabrication process which translates to phase uncertainty in the optical signal [3]. Regardless the choice of material, these waveguides often have propagation losses greater than  $3 \times 10^5$  dB/km (or 3 dB/cm) [4]. Comparing this number to usual losses in a fiber optic cable shown in Figure 1, it is evident slab dielectric waveguides are only suitable for mm or cm sized devices. To ensure minimal losses, the height of the  $\text{SiO}_2$  cladding (see Figure 3) must be at least  $1 \mu\text{m}$  so that the intensity has sufficient distance to exponentially decay before the substrate is reached. The height/width ratio of the waveguide core must be carefully chosen to ensure single mode propagation and minimal losses. The sensitivity of this ratio is clear from the data in Figure 3 (data taken from source [5]).



Width (nm)	Experimental propagation loss (dB/cm)	Theoretical substrate leakage (dB/cm)
400	$34 \pm 1.7$	3.6
440	$9.5 \pm 1.8$	1.8
450	$7.4 \pm 0.9$	1.7
500	$2.4 \pm 1.6$	1.1

Figure 3 (Right) Propagation losses for waveguides with various core widths, assuming a core height of 220 nm and cladding thickness of  $1 \mu\text{m}$ .

A Si-based WDM requires the following elements: Si waveguides, integrated germanium photodetectors, and a modulator. In the literature, there are at least three modulators that have been successfully implemented to achieve multiplexing/demultiplexing on Si-based PICs: (i) an arrayed waveguide grating, (ii) a Mach-Zehnder interferometer, and (iii) a ring resonator. The following portion of this essay will discuss the physics behind these three modulators.

### *Arrayed waveguide grating*

An arrayed waveguide grating (AWG) can be used to split the signal into its component frequencies. Figure 4 shows a 40-channel demultiplexer with a monolithically integrated SiN AWG, from source [6]. The AWG functions as follows: first, the input signal which contains a superposition of frequencies is allowed to propagate as an unconfined spherical wave front in the "free propagation region" (FPR) labeled " $n_s$ " on Figure 4 (left) or "SiN" on Figure 4 (right). The light is then collected in a bundle of equally-spaced waveguides, and guided around bends of

different length ( $\Delta l$ ), causing the separate paths to undergo differential phase shifts of  $n_{eff}\Delta l$  upon arriving at the second FPR. In the second FPR, the light interferes at the entries of the output waveguides in such a way that each channel only receives a certain wavelength of light. The AWG diffraction equation is:

$$n_{eff}\Delta l + n_s\Lambda(\sin \theta_{inc} + \sin \theta_d) = m\lambda \quad (1)$$

where  $\theta_{inc}$  is the angle of incidence into the first FPR, and  $\theta_d$  is the angle of incidence into the second FPR. We can substitute  $\lambda = \frac{2\pi c}{\omega}$ , take a derivative with respect to  $\omega$ :

$$\frac{d\theta_d}{d\omega} \approx \frac{n_g\Delta l}{n_s\omega\Lambda \cos \theta_d} = \frac{2\pi c n_g m}{n_s n_{eff} \omega^2 \Lambda \cos \theta_d} \quad (2)$$

where the device is carefully designed so differential path lengths  $\Delta l = m \lambda_0/n_{eff}$ .

From equation (2), it is clear that the angular dispersion spatially separates the frequencies at the entries of the output waveguides. In this manner, the broadband signal is demultiplexed into its component frequencies.

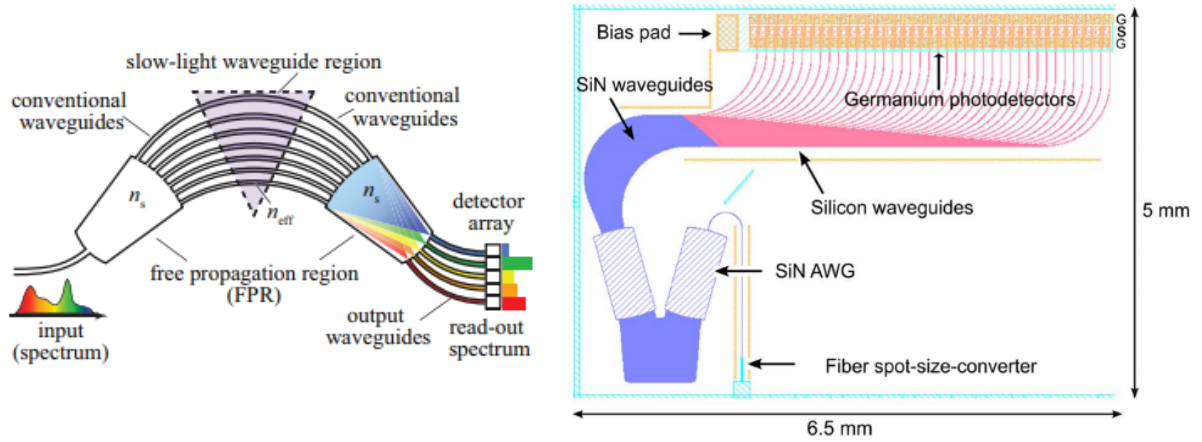


Figure 4: (Left) general schematic of an AWG, figure taken from source [7]. (Right) 40-channel demultiplexer using a SiN AWG, figure taken from source [6].

### *Mach-Zehnder interferometer*

A two channel Mach-Zehnder interferometer (MZI) demultiplexer has been realized by Chen et al., also integrated into a Si-based PIC [8]. Four years later, the MZI model for multiplexing on Si chips was extended to include 8 channels [9]. Even though Chen's device only has two channels, it is quite novel because this WDM is polarization insensitive. The optical confinement in slab dielectric waveguides typically causes large optical birefringence, which makes polarization-insensitive circuit elements in these PICs a large challenge. The researchers were able to cancel the polarization-dependent phase shift caused by the waveguide's birefringence with two tricks: one, using waveguides with a square cross section, and two, choosing the lengths of the delay-line waveguides such that the total accumulated phase  $n * l$  negates the effect of the different  $n$

(from birefringence of the waveguide) has on the phase of the two paths. It should be noted, for the MZI to work, a phase difference is needed at the end, so  $n_1 * l_1 \neq n_2 * l_2$ , however, the difference caused by birefringence can still be negated.

A MZI's operation is mathematically analogous to a classical optical MZ interferometer, but the coupling between the two paths is achieved through couplers rather than beam splitters. The input signal containing multiple wavelengths shown in Figure 5 (b) comes into channel 1 of Figure 5 (a). There is a coupling between the  $L_1$  and  $L_2$  waveguides which acts as a grating. The grating is resonant with the wavelength that it drops/adds, such as the center wavelength in Figure 5 (c). In the drop operation, this resonant wavelength is reflected, and leaves the MZI through channel 2. The non-resonant wavelengths are then transmitted through channel 4, missing the dropped frequency (Figure 5 (d)). In an ideal drop operation, no light will leave through channel 1 or channel 3. To add wavelengths, the input again enters through channel 1. The signal to be added, which must be resonant with the grating, enter through channel 3, and the multiplexed signal is transmitted through channel 4.

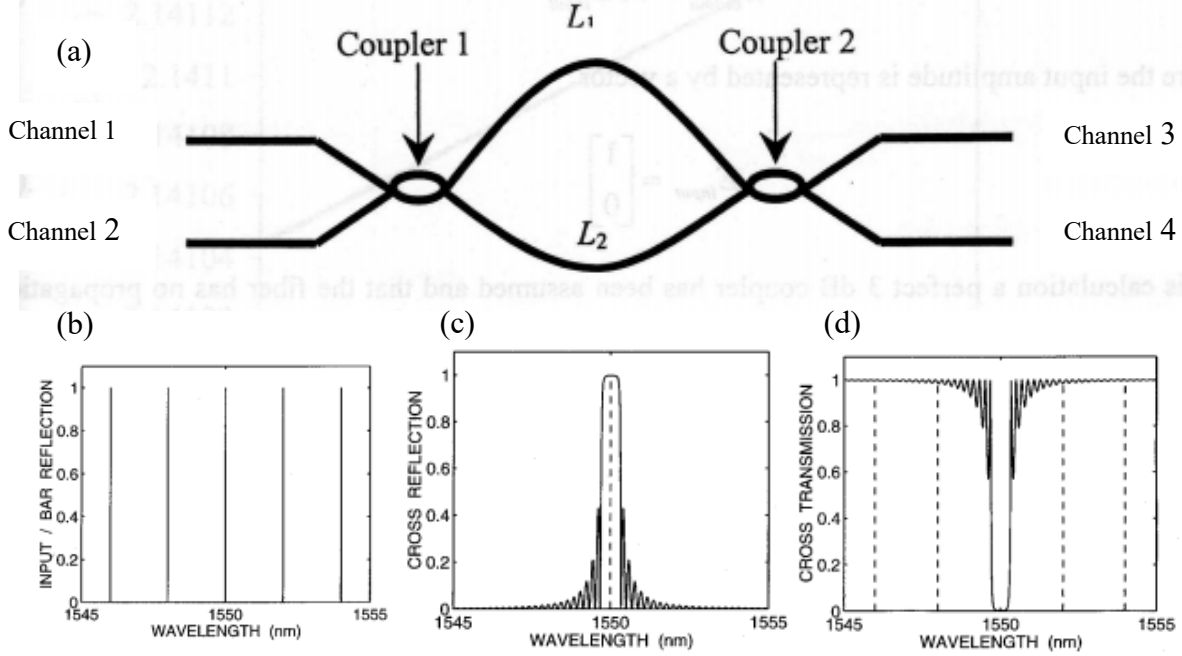


Figure 5: (a) Schematic of a 2-channel MZI WDM, from source [10] (b-d) Example of an MZI drop operation, from source [11].

Mathematically, the relationship between the input and output electric fields can be expressed with a matrix formalization of the sequential transformations between the input and output channels

$$E_{output} = (M_{coupler} M_{phaseshift} M_{coupler}) E_{input} \quad (3)$$

where  $M_{phaseshift}$  adds a phase shift simply from the propagation along  $L_1$  and  $L_2$ :  $\phi = \frac{2\pi n_{eff}}{\lambda} (L_1 - L_2)$ , and  $M_{coupler}$  rotates the field by an angle  $\theta = \kappa z$ . Here,  $\kappa$  is the 'coupling

coefficient' that depends on the spacing between the two waveguides labeled  $L_1$  and  $L_2$  in Figure 5 (a), and  $z$  is the coupler length [10].

As shown in Figure 6 (right), a series of MZIs can be connected to make a multiplexer with more than two channels. In this case, the WDM has 8 channels.

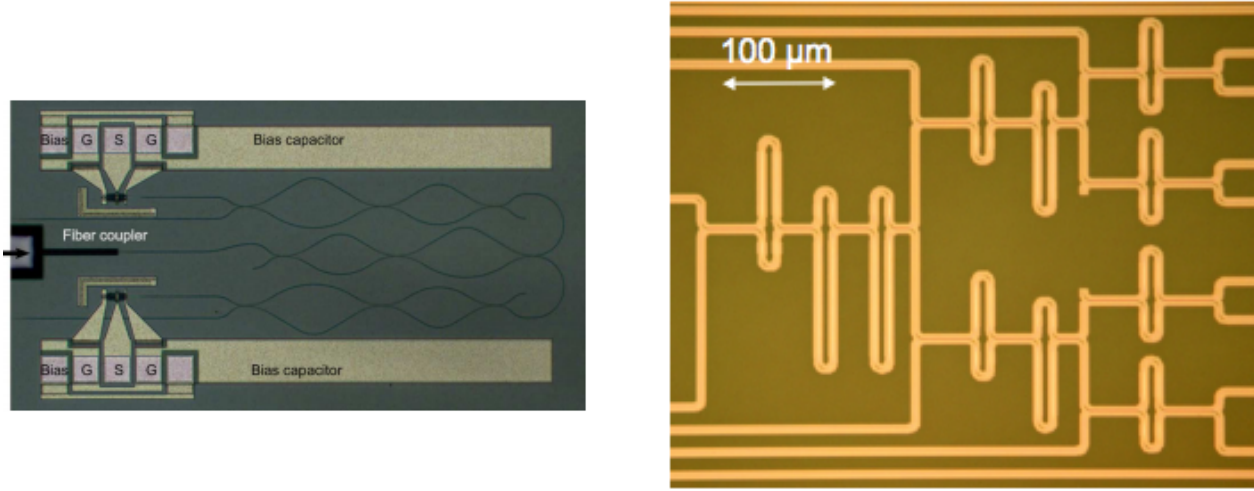


Figure 6: Si-based MZI multiplexing circuits. (Left) The 2-channel polarization insensitive WDM, from source [8]. (Right) A much smaller 8-channel WDM from source [9].

### Ring Resonator

The ring resonator's approach to wavelength addition/subtraction has fundamental similarities to the MZI WDM. In ring resonators, the optical signal makes multiple trips around a ring-shaped waveguide. The ring's circumference is an integer multiple a certain wavelength that is resonant with the ring. Similar to the MZI, the coupling between two or more ring waveguides can act like a grating to add/drop wavelengths.

To understand this in more depth, we start with the simple all-pass filter shown in Figure 7 (a). When the input light meets the resonant conditions of the ring (that is,  $\lambda = \frac{L n_{eff}}{m}$ ), the light will couple into the ring and travel around it (where  $L$  is the circumference of the ring). The ratio of the field that is transmitted is given by:

$$T_n = \frac{I_{pass}}{I_{input}} = \frac{a^2 - 2racos\phi + r^2}{1 - 2arcos\phi + (ra)^2} \quad (4)$$

where  $\phi = \frac{2\pi n_{eff}}{\lambda} L$  is the single pass phase shift (same as  $\phi$  in MZI above),  $a^2$  is simply the power attenuation from the losses of making a roundtrip,  $r$  is the self-coupling coefficient, and  $k$  is the cross-coupling coefficient. These coefficients represent the power splitting between the waveguide and the ring. The conservation of energy requires  $k^2 + r^2 = 1$ .

It is quite simple to extend this picture to include another waveguide, as shown in Figure 7 (b). We add another set of coupling coefficients to represent coupling between the ring resonator and the add/drop waveguide, so now we have  $k_1, k_2$  and  $r_1, r_2$ . A specific wavelengths can be dropped by coupling into a ring of correct circumference, and exit through the upper “add/drop” waveguide in Figure 7. Similarly, a wavelength can be added by entering through the opposite end of the “add/drop” waveguide, couple to the ring, and exit into the full optical signal. This coupling into and out of the ring is represented by transmission functions of the pass and drop ports:

$$T_d = \frac{I_{\text{drop}}}{I_{\text{input}}} = \frac{(1 - r_1^2)(1 - r_2^2)a}{1 - 2r_1r_2a \cos \phi + (r_1r_2a)^2}, \quad T_p = \frac{I_{\text{pass}}}{I_{\text{input}}} = \frac{r_2^2a^2 - 2r_1r_2a \cos \phi + r_1^2}{1 - 2r_1r_2a \cos \phi + (r_1r_2a)^2}$$

Plotting the transmission as a function of  $\phi$  (which depends on wavelength), we see minima occurs when  $k_1 = k_2$ .

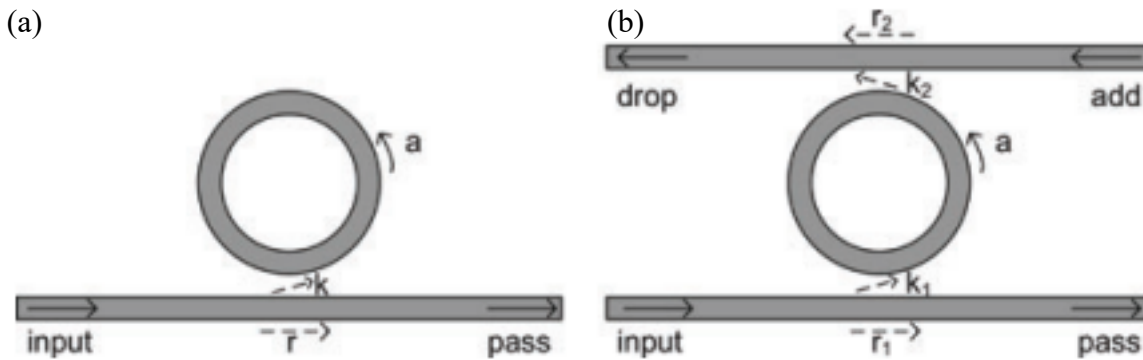


Figure 7: Schematic of a ring resonator’s add/drop function, taken from source [12].

In conclusion, this essay has summarized the working physics behind 3 ways of multiplexing in PICs: the arrayed waveguide grating, the Mach-Zehnder interferometer, and the ring resonator.

References:

- [1] Coffey, Joe. Introduction to Wave Division Multiplexing.  
[www.bicsi.org/pdf/Regions/southcentral/WaveDivisionMultiplexing.pdf](http://www.bicsi.org/pdf/Regions/southcentral/WaveDivisionMultiplexing.pdf)
- [2] Dong, Po, et al. "Silicon photonic devices and integrated circuits." *Nanophotonics* 3.4-5 (2014): 215-228.
- [3] Dong, Po. "Silicon photonic integrated circuits for wavelength-division multiplexing applications." *IEEE Journal of Selected Topics in Quantum Electronics* 22.6 (2016): 370-378.
- [4] Boeck, Robert. "Silicon Ring Resonator Add-Drop Multiplexers." Master's thesis, The University of British Columbia, Oct. 2011.
- [5] W. Bogaerts. "Nanophotonic Waveguides and Photonic Crystals in Silicon-on-Insulator." PhD thesis, Universiteit Gent, Apr. 2004
- [6] Chen, Long, et al. "Monolithically integrated 40-wavelength demultiplexer and photodetector array on silicon." *IEEE Photonics Technology Letters* 23.13 (2011): 869-871.
- [7] Shi, Zhimin, and Robert W. Boyd. "Fundamental limits to slow-light arrayed-waveguide-grating spectrometers." *Optics express* 21.6 (2013): 7793-7798.
- [8] Chen, Long, et al. "Compact integrated polarization-insensitive two-channel receiver on silicon." *IEEE Photonics Technology Letters* 23.15 (2011): 1073-1075.
- [9] Horst, Folkert, et al. "Cascaded Mach-Zehnder wavelength filters in silicon photonics for low loss and flat pass-band WDM (de-) multiplexing." *Optics express* 21.10 (2013): 11652-11658.
- [10] Syahriar, Ary. "Mach Zehnder Interferometer for Wavelength Division Multiplexing." KOMMIT (2002).
- [11] Erdogan, Turan, et al. "Integrated-optical Mach-Zehnder add-drop filter fabricated by a single UV-induced grating exposure." *Applied optics* 36.30 (1997): 7838-7845.
- [12] Bogaerts, Wim, et al. "Silicon microring resonators." *Laser & Photonics Reviews* 6.1 (2012): 47-73.